# Morphological image analysis for classification of gastrointestinal tissues using optical coherence tomography

P. Beatriz Garcia-Allende<sup>1,2,3</sup>, Iakovos Amygdalos³, Hiruni Dhanapala⁴, Robert D. Goldin³, George B. Hanna³ and Daniel S. Elson<sup>1,3</sup>

#### ABSTRACT

Computer-aided diagnosis of ophthalmic diseases using optical coherence tomography (OCT) relies on the extraction of thickness and size measures from the OCT images, but such defined layers are usually not observed in emerging OCT applications aimed at "optical biopsy" such as pulmonology or gastroenterology. Mathematical methods such as Principal Component Analysis (PCA) or textural analyses including both spatial textural analysis derived from the two-dimensional discrete Fourier transform (DFT) and statistical texture analysis obtained independently from center-symmetric auto-correlation (CSAC) and spatial grey-level dependency matrices (SGLDM), as well as, quantitative measurements of the attenuation coefficient have been previously proposed to overcome this problem. We recently proposed an alternative approach consisting of a region segmentation according to the intensity variation along the vertical axis and a pure statistical technology for feature quantification. OCT images were first segmented in the axial direction in an automated manner according to intensity. Afterwards, a morphological analysis of the segmented OCT images was employed for quantifying the features that served for tissue classification. In this study, a PCA processing of the extracted features is accomplished to combine their discriminative power in a lower number of dimensions. Ready discrimination of gastrointestinal surgical specimens is attained demonstrating that the approach further surpasses the algorithms previously reported and is feasible for tissue classification in the clinical setting.

Keywords: Medical optics and biotechnology, spectroscopy, tissue diagnostics, computer aided diagnosis

## 1. INTRODUCTION

The ability of optical coherence tomography (OCT) to accomplish noninvasive cross-sectional imaging in biological systems<sup>1</sup> provides it with enormous potential to be employed for "optical biopsy" in diverse disciplines including its traditional use in ophthalmology as well as many other emerging medical applications such as cardiology, dermatology, and oncology. Its potential in gastroenterology is also poised to be realized in the coming years, since it could solve the limitations of current clinical management of patients with gastrointestinal diseases in terms of the small tissue fraction sampled during standard endoscopic examinations.

In hospital histopathology departments there is an immense workload and time pressure. Sampling, sectioning and staining of tissue specimens are required, and then microscopic evaluation follows to provide diagnostic information just at one location. Multiple fixed and unfixed tissue specimens are processed and reported on and lab resources and staff time must be used as economically as possible. Reporting must be completed by specific deadlines so that results can be discussed in multi-disciplinary meetings and made available to patients

Further author information: (Send correspondence to P.B. Garcia-Allende)
P.B. Garcia-Allende: E-mail: pb.garcia-allende@helmholtz-muenchen.de, Telephone: 49 (0)89 3187 4191

Optical Coherence Tomography and Coherence Domain Optical Methods in Biomedicine XVI, edited by Joseph A. Izatt, James G. Fujimoto, Valery V. Tuchin, Proc. of SPIE Vol. 8213, 821328 © 2012 SPIE · CCC code: 1605-7422/12/\$18 · doi: 10.1117/12.907835

Proc. of SPIE Vol. 8213 821328-1

<sup>&</sup>lt;sup>1</sup>Hamlyn Centre for Robotic Surgery, Institute of Global Health Innovation, Imperial College London, London SW7 2AZ, UK;

<sup>&</sup>lt;sup>2</sup> Current address: Institute for Biological and Medical Imaging, Helmholtz Zentrum M $\ddot{u}$ nchen, Ingolst $\ddot{a}$ dter Landstra $\beta$ e 1, D-85764 Neuherberg, Germany;

<sup>&</sup>lt;sup>3</sup>Department of Surgery and Cancer, Faculty of Medicine, Imperial College London, St Mary's Hospital, London W2 1NY, UK;

<sup>&</sup>lt;sup>4</sup>Imperial College Healthcare NHS Trust, St Mary's Hospital, London W2 1NY, UK

and clinicians. A computer aided diagnosis (CAD) using OCT would be of enormous benefit since it could even avoid the need for tissue biopsies. However, this implies that OCT images must be automatically (non visually) assessed and a quick and reproducible tissue classification approach needs to be developed.

In ophthalmology, this automated classification was accomplished by extracting thickness and size measures from the OCT images, but defined layers are usually not observed in non-ophthalmic imaging. Consequently, disease quantification has traditionally relied on a loss of tissue structure that could be measured through textural analysis in OCT images using smoothness, coarseness, homogeneity, etc.<sup>2-6</sup> These analyses can be classified in terms of the approach employed for the quantification of the features that serve for tissue classification. Some of them make use of the two-dimensional discrete Fourier transform (DFT),<sup>3</sup> since DFT features can detect texture periodicity and orientation, while others employ more sophisticated approaches such as using spatial gray-level dependence matrices (SGLDM)<sup>2,5</sup> or center-symmetric auto-correlation (CSAC) textural features.<sup>4</sup> The combination of these approaches has shown promising results in disease detection but all of them are subject to the identification of an appropriate region of interest (ROI) for feature quantification. Additionally, further processing of the combined features using principal components analysis (PCA)<sup>7</sup> is required to increase the discriminative power. In some cases further processing of the scores of the principal components are used as variables for linear discriminant analysis (LDA),<sup>5</sup> and only then is reliable classification achieved.

Alternative approaches to the aforementioned mathematical methods employ quantitative measurements of the attenuation coefficient,  $(\mu_t)$ , describing the decay of detected light intensity with depth.<sup>8,9</sup> These are based on variations of the measured backscattering between normal and tumor tissues and even at various stages of tumor genesis.<sup>8</sup> These differences, however, can be obscured by system artifacts preventing reliable diagnostics.<sup>8</sup>

We recently proposed a two-step methodology to overcome these limitations.<sup>10</sup> OCT images were first segmented in the axial direction in an automated manner according to intensity, though avoiding the uncertainty regarding the identification of the most appropriate ROI for image parameter extraction. Afterwards, a morphological analysis of the segmented images was employed for feature quantification. In this study it will be demonstrated that this approach surpasses textural algorithms, provides independency from system artifacts and no further improvement is achieved with a posterior PCA processing of the extracted features, since they reliably serve on their own for gastrointestinal tissue classification in the clinical setting.

#### 2. MATERIALS AND METHODS

## 2.1 OCT imaging of gastrointestinal surgical specimens

A commercial swept-source (SS) OCT system OCS1300SS (Thorlabs Incorporated, Newton, New Jersey) was employed to image freshly-excised specimens of gastrointestinal tissues. This data was collected at St Marys Hospital, Paddington, London from February to September 2010 and it included patients undergoing elective gastrointestinal surgery, who where able to provide written informed consent. Specimens were collected from theaters in warm normal saline (0.9% sodium chloride) as soon as they were excised and immediately taken to the histology lab. There, they were gently rinsed exposing the mucosa and any lesions. In order to stabilise them for imaging and working of sites of interest, specimens were pinned onto corkboards. Specimens from gastrointestinal surgery were generally quite large and much thicker than the penetration depth of the OCT beam. Therefore, they did not require any special mounting and were imaged directly on the corkboard. After imaging was complete (within 30 minutes of resection), tissues were fixed with 10% formalin and returned to pathology for routine histological processing. A total of 35 sites that were 3x3 mm in size were imaged. Nine of them corresponded to tumor sites (belonging to 7 different patients), while the remaining images included stomach (20 sites from 9 patients), and oesophagus (6 sites from 6 patients). A 3D volume data set (C-scan) was obtained per imaged site. The OCT software always generated data to a fixed depth of 3 mm, regardless of the on-screen depth set by the user, which was for viewing purposes only. Consequently, the other two dimensions were fixed to 3 mm length to obtain a cube-shaped C-scan. The lateral resolution was set to 512 pixels which implies that each C-scan consists of 512 transverse OCT images (B-scans). As the axial resolution of the system was also fixed at 512 pixels, the resulting OCT images contains 512 axial scans (A-scans) each.

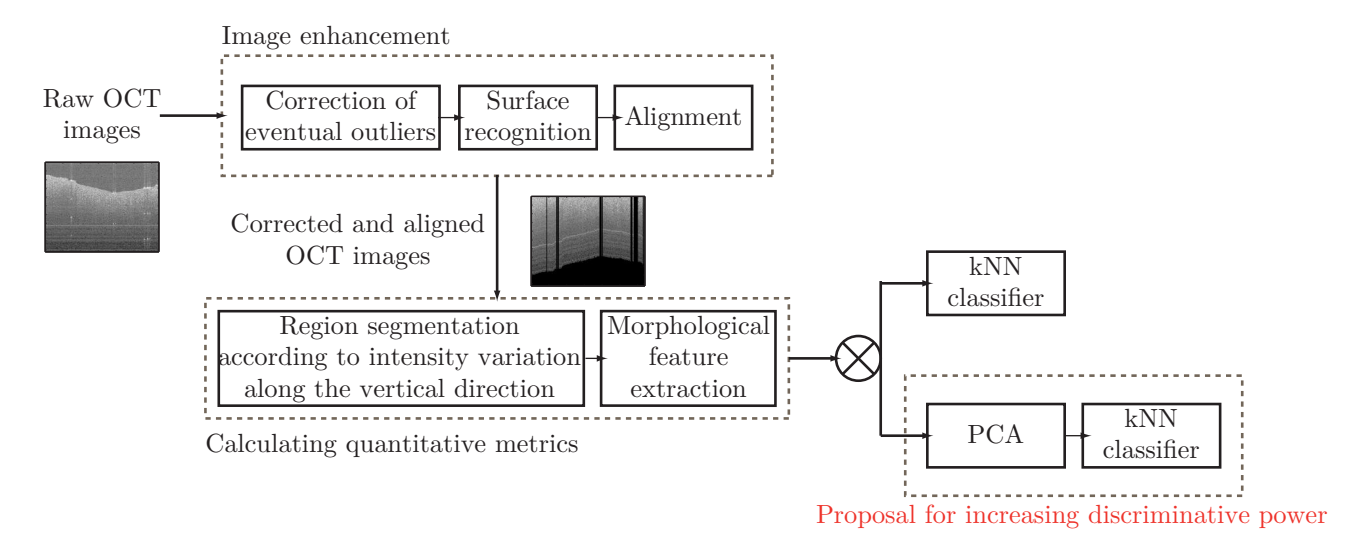


Figure 1. Flow diagram of OCT image-processing stages and alternatives.

### 2.2 Image classification using morphological features-fed principal component analysis

Matlab 7.9.0.529 (R2009b) was utilized off-line for image processing. The first step in processing consisted of a region segmentation of every OCT image according to the intensity variation along the vertical direction employing the k-means method. The employment of such a segmentation strategy avoids the necessity of previously known information about the tissue structure as in and, therefore, makes the approach more extensible for tissue classification in other medical applications. To study the intensity distribution of each segmented region, the first four statistical moments (mean, standard deviation, skewness and kurtosis) of the intensity values per region were computed, and a fifth feature was created from the relative area of the segmented region with respect to the total area of the B-scan. Accordingly the total number of extracted features from the OCT images for tissue classification was five times the number of segmented regions. Finally, a kNN classification was applied to the extracted features to understand the relationship between the image parameters, and to form predictions for newly acquired data.

For analysis of tissue discrimination performance all data were randomly divided into three nonoverlapping sets. Two of these sets were employed as a training set for the kNN classifier and the other was employed as validation set to compute accuracy, sensitivity, specificity, negative predictive value (NPV) and positive predictive value (PPV). These measures were obtained based on the ability to discriminate a given tissue type in this validation set from all other categories evaluated. This procedure was repeated three times for all possible permutations of training and test sets and reported measures were the averages of these three executions. This threefold cross validation procedure was replicated for a varying number of segmented regions, to study the dependence of the tissue discrimination capability of the approach on the number of segmented regions chosen. Furthermore, an additional PCA processing of the extracted features as in<sup>5</sup> is included in this study, and its provided increase in discriminative power is estimated through a cross-validation procedure as described for the raw extracted morphological features. A schematic of the whole image enhancement and interpretation is depicted in Figure 1 and a more detailed description of the image correction process that comprises reflection artifact removal and surface detection and alignment, and the employment of the kNN classifier to understand the relationship between the image parameters can be found in the previous paper.<sup>10</sup>

## 3. RESULTS AND DISCUSSION

The extracted metrics initially proposed for distinguishing upper gastrointestinal pathologies, i.e. through morphological analysis of the segmented OCT images, are shown graphically for each tissue type in Figure 2. As anticipated by alternative approaches employing quantitative measurements of the attenuation coefficient, <sup>8,9</sup> region segmentation highlights the steeper decrease of the region mean intensity from tumor. This implies that

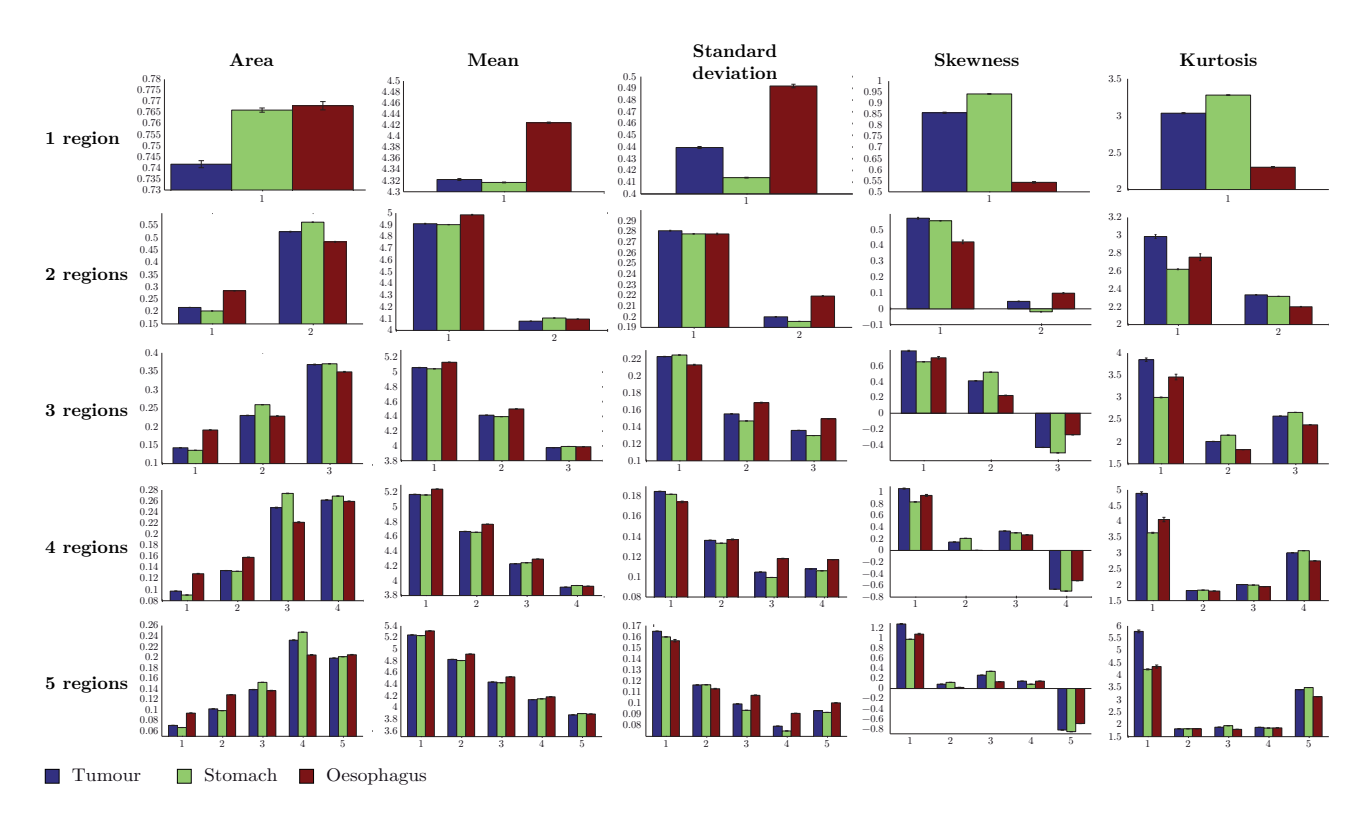


Figure 2. Morphological metric values (mean±SEM) for the three different tissue types: tumor, stomach and oesophagus.

tumor mean intensity is higher than stomach mean intensity for superficial regions while the opposite situation is encountered for deep regions in the axial direction. Oesophagus appears to be mostly brighter (higher mean intensities) in all regions. However, other metrics such as the standard deviation or skewness seem to be more suitable for distinguishing the different pathologies since they provide, as depicted in Fig. 2, larger statistical differences. Still, these differences look insufficient to individually provide reliable sensitivity and specificity for identifying tumor from stomach and oesophagus and the employment of further analysis as PCA or linear discriminant analysis (LDA)<sup>5</sup> to combine their discriminative power in a lower number of dimensions seems necessary. The validity of this assumption for PCA is demonstrated in Figure 3, which graphically depicts an evaluation of the principal components as classifiers showing much greater statistical differences than in the initial image classification features depicted in Fig. 2.

Figure 4 qualitatively compares the performance of the proposed approach, i.e. subsequent PCA of the morphological features, as a function of the number of segmented regions chosen. A tendency to group is observed in the scatter plots when the first three components are maintained that, as depicted in Fig. 3, contain most of the variance present in the initial image parameters. This indicates the ability of the approach to coarsely differentiate diagnostic categories. The degree of clustering within the same tissue type and the separation among types seem to increase as the number of segmented regions increases but this qualitative assumption needs to be confirmed using specificity and sensitivity values, i.e. through the employment of the kNN classifier to predict unknown new data and to establish a comparison with the prediction without PCA. Sensitivity and specificity values are compared with those obtained directly using morphological image parameters as classifiers. Since the overlap among these categories is also noticeable, a value of k = 1 was selected because larger values of k reduced the effect of noise on the classification, but also made boundaries between classes less distinct.<sup>6</sup>

The result of this performance evaluation is summarized in Table 1 and confirms that using more than 2 segmented regions does not provide a further improvement in the accuracy. In addition, it would imply an increase in the computational load because five features are extracted per segmented region. In fact for six regions, tissue identification capabilities start to decrease dramatically, presumably due to the noisy results of

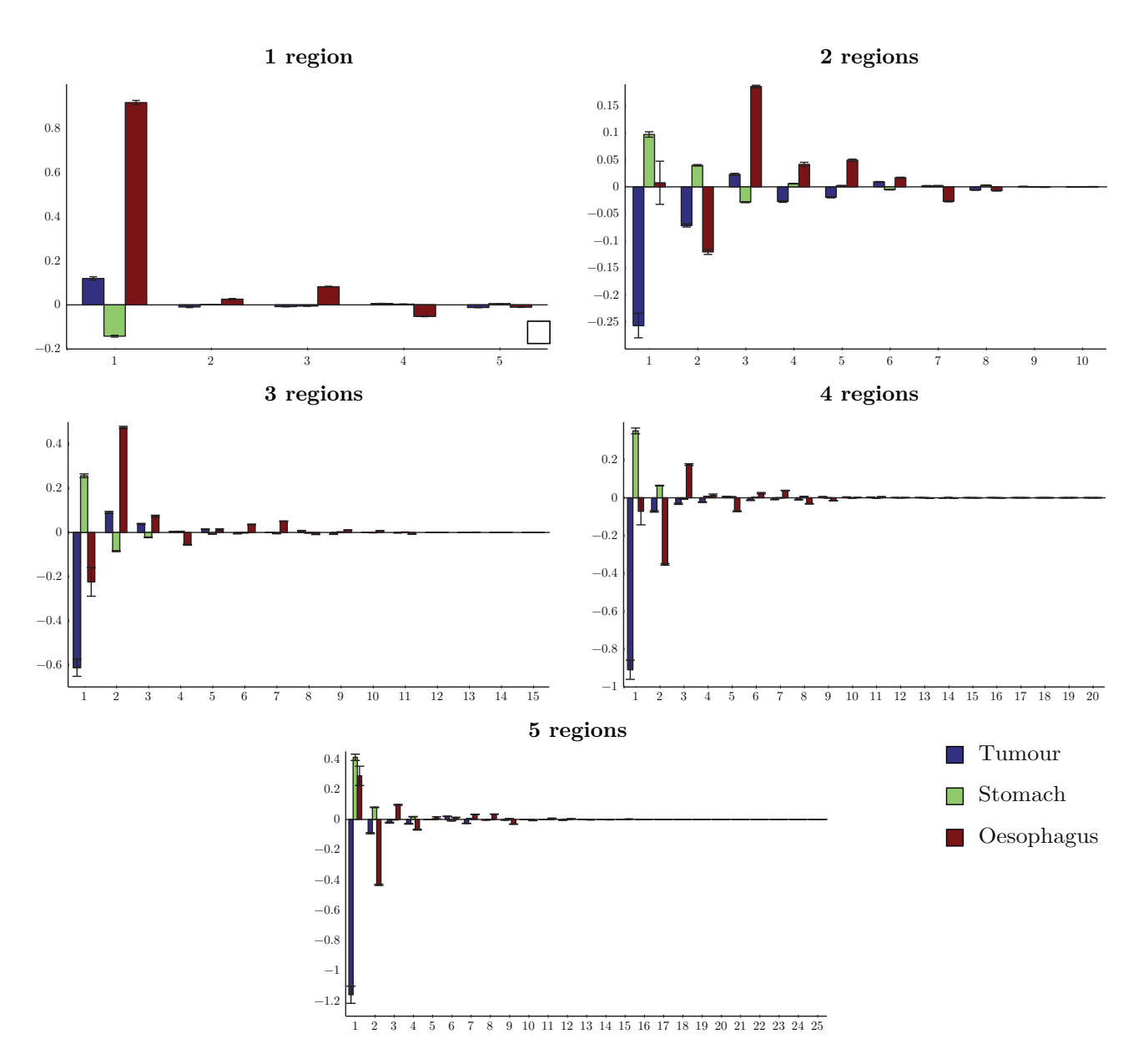


Figure 3. Metric values (mean±SEM) when principal component analysis was applied to potential image classification features and images were divided into a different number of segmented regions, for the three different tissue types: tumor, stomach and oesophagus.

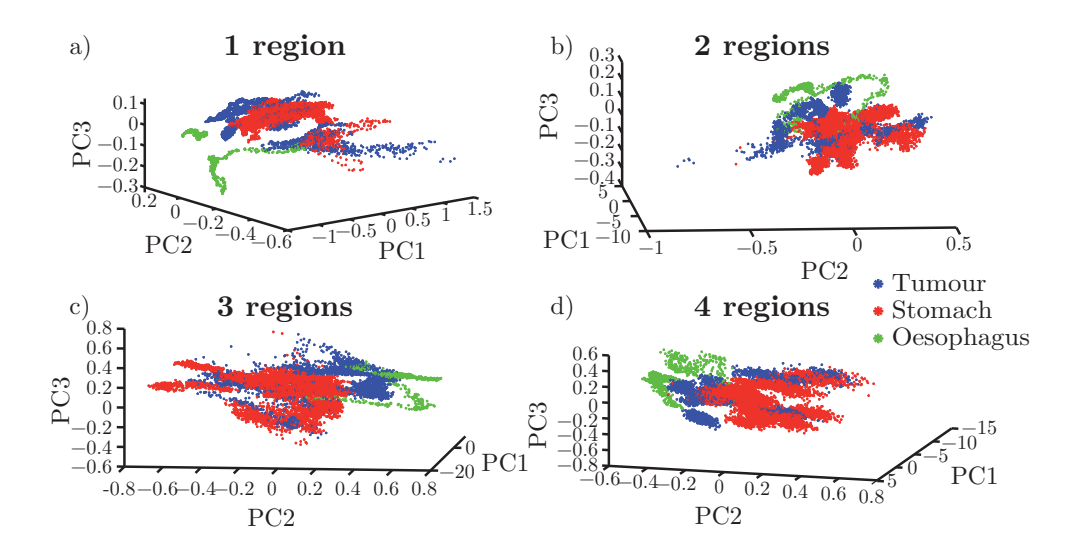


Figure 4. Grouped scatter plots for the distinct gastrointestinal tissues depending on the number of segmented regions.

Table 1. K-nearest neighbour classification results for varying number of segmented regions.

Number of segmented regions	Sensitivity	Specificity	PPV	NPV	Accuracy
1	99.5%:	99.0%:	97.3%:	99.8%:	99.2%:
	99.8%:100%	98.7%:98.8%	99.4%:86.4%	99.7%:100%	99.4%:98.9%
2	99.9%:	99.8%:	99.6%:	99.9%:	99.9%:
	100%:100%	99.7%:100%	99.6%:99.6%	100%:100%	99.9%:100%
3	99.9%:	99.8%:	99.5%:	100%:	99.9%:
	100%:100%	99.8%:100%	99.9%:98.6%	100%:100%	100%:100%
4	99.9%:	99.8%:	99.5%:	100%:	99.9%:
	100%:100%	99.9%:99.9%	99.9%:98.1%	100%:100%	100%:99.9%
5	99.9%:	99.7%:	99.9%	100%:	99.8%:
	100%:100%	100%:99.7%	100%:96.0%	100%:100%	100%:99.7%
6	95.5%:	78.1%:	53.0%:	97.9%:	77.2%:
	89.1%:99.6%	83.4%:78.2%	91.7%:26.1%	78.8%:100%	87.2%:79.7%

the segmentation process. Classification measures are provided per diagnostic category from all others, i.e. an accuracy of 99.2%:99.4%:98.9% indicates that accuracy in tumour, stomach and oesophagus identification are 99.2%, 99.4% and 98.9%, respectively. Table 2 therefore compares the sensitivity and specificity values attained with two segmented regions with previous approaches proposed for tissue classification using OCT. Obtained classification measures reinforce the significant improvement attained using morphological features as compared to textural. PCA post-processing of the extracted features is required to achieve reliable classification for the clinical setting when textural approaches are followed. In spite of the larger statistical differences attained with the PCA processing of the extracted morphological features, their further processing with the KNN classifier already provides reliable tissue categorization in clinical settings and slightly further enhancement is attained by the intermediate PCA stage. The further PCA processing of the extracted features aids in reducing the variable dimensions, i.e. it reduces the spatial complexity for in vivo classifications but it is not compulsory as compared to textural to increase the discriminative power and provide trustworthy tissue classification.

Table 2. Quantitative comparison between morphological and textural approaches for feature quantification of OCT images in the classification of gastrointestinal tissues.

Feature extraction approach	Sensitivity	Specificity	PPV	NPV	Accuracy
Morphological (2 regions)	99.9%:	99.8%:	99.6%:	99.9%:	99.9%:
	100%:100%	99.7%:100%	99.6%:99.6%	100%:100%	99.9%:100%
Morphological (2 regions) + PCA	100%: 99.9%:100%	99.8%: 100%:98.9%	99.51%: 100%:86.9%	100%: 99.9%:100%	99.9%: 100%:98.9%
DFT + SGLM	91.1%:	69.3%:	50.1%:	95.8%:	74.9%:
	83.2%:100%	85.6%:61.1%	92.2%:16.4%	71.2%:100%	84.0%:63.9%
DFT + SGLM	96.1%:	85.6%:	69.7%:	98.5%:	88.3%:
+ PCA	93.9%:100%	92.2%:70.5%	96.1%:20.6%	88.0%:100%	93.3%:72.6%
DFT + CSAC	96.2%:	50.9%:	40.6%:	97.6%:	62.5%
	78.9%:99.9%	83.8%:53.0%	90.9%:14.0%	65.8%:100%	80.5%:56.3%
$\mathrm{DFT} + \mathrm{CSAC} + \mathrm{PCA}$	95.9%:	86.0%:	70.27%:	98.4%:	88.6%:
	93.8%:99.9%	91.3%:69.9%	95.7%:20.3%	87.7%:100%	93.0%:72.1%

#### 4. CONCLUSIONS

A principal component analysis to increase the discriminative power of a previously reported two-step methodology for extracting features from OCT images that serve for tissue classification is proposed in this study. OCT images were first segmented in the axial direction in an automated manner according to intensity, avoiding uncertainty in the identification of the most appropriate region of interest for feature computation. Afterwards, a morphological analysis of the segmented OCT images was employed for feature quantification. Sensitivity and specificity values were obtained in a cross validation procedure to eliminate the dependance on the employed data sets and demonstrate that the approach surpasses previous alternatives and reliably provides gastrointestinal tissue classification in a clinical setting. A subsequent principal component analysis of the morphological image parameters was utilized to combine the discriminative power of the morphological image parameters in a lower number of dimensions, though simultaneously enhancing the accuracy and the time performance of the approach in the classification stage. However, sensitivity and specificity enhancement were not as relevant as in other alternatives methodologies found in the literature, i.e. textural features, though confirming the enhanced behaviour attained using morphological features as compared to textural. Additionally, the blind region segmentation process avoids the necessity of previously known information about the tissue structure for determining the most appropriate region of interest for image feature quantification. Accordingly the extendability of the approach for future tissue classification in other OCT applications is in this way greatly enhanced. For this reason, we are currently imaging further gastrointestinal tissues to confirm that the deviations that are investigated as disease marker are greater than interpatient variation, as well as tissue specimens from urological operations to demonstrate the validity of the approach in another medical application.

#### ACKNOWLEDGMENTS

Funding is gratefully acknowledged from the ERC grant StG 242991. This work was also partly funded by the National Physical Laboratory, Teddington, Middlesex, UK.

## REFERENCES

[1] D. Huang, E.A. Swanson, C.P. Lin, J.S. Schuman, W.G. Stinson, W. Chang, H.R. Hee, F. Flotte, K. Gregory, C.A. Puliafito, and J.G. Fujimoto, "Optical coherence tomography," Science **254**, 1178–1181 (1991).

- [2] K.W. Gossage, J.J. Rodriguez, and J.K. Barton, "Texture analysis of optical coherence tomography images: feasibility for tissue classification," J. Biomed. Opt. 8, 570–575 (2003).
- [3] K.W. Gossage, C.M. Smith, E.M. Kanter, L.P. Hariri, A.L. Stone, J.J. Rodriguez, S.K. Williams, and J.K. Barton, "Texture analysis of speckle in optical coherence tomography images of tissue phantoms," Phys. Med. Biol. **51**, 1563–1575 (2006).
- [4] X. Qi, M.V. Sivak Jr., G. Isenberg, J.E. Willis, and A.M. Rollins, "Computer-aided diagnosis of dysplasia in Barrett's esophagus using endoscopic optical coherence tomography," J. Biomed. Opt. 11, 0440101–04401010 (2006).
- [5] Y. Chen, A.D. Aguirre, P.L. Hsiung, S.W. Huang, H. Mashimo, J.M. Schmitt, and J.G. Fujimoto, "Effects of axial resolution improvement on optical coherence tomography (OCT) imaging of gastrointestinal tissues," Opt. Express 16, 2469–2485 (2008).
- [6] X. Qi, Y. Pan, S.V. Sivak Jr., J.E. Willis, G. Isenberg, and A.M. Rollins, "Image analysis for classification of dysplasia in Barrett's esophagus using endoscopic optical coherence tomography," Biomedical Optics Express 1, 825–847 (2010).
- [7] I.T. Jolliffe, Principal Component Analysis (Springer, 2nd ed., 2002).
- [8] E.C. Cauberg, D.M. de Bruin, D.J. Faber, T.M. de Reijke, M. Visser, J.J. de la Rosette, and T.G. van Leeuwen, "Quantitative measurement of attenuation coefficients of bladder biopsies using optical coherence tomography for grading urothelial carcinoma of the bladder," J. Biomed. Opt. 15, 0660131–0660136 (2010).
- [9] K. Barwari, D.M. de Bruin, E.C. Cauberg, D.J. Faber, T.G. van Leeuwen, H. Wijkstra, J.J. de la Rosette, and M.P. Laguna, "Advanced diagnostics in renal mass using optical coherence tomography: A preliminary report," J. Endourol. **25**, 311–315 (2011).
- [10] P.B. Garcia-Allende, I. Amygdalos, H. Dhanapala, R.D. Goldin, G.B. Hanna, and D.S. Elson, "Morphological analysis of optical coherence tomography images for automated classification of gastrointestinal tissues," Biomedical Optics Express 2, 2821–2836 (2011).
- [11] R. Ghanadesikan, Methods for Statistical Data Analysis of Multivariate Observation (John Wiley & Sons, New York, 1997).
- [12] A. Barui, P. Banerjee, R. Patra, R.K. Das, S. Dhara, P.K. Dutta, and J. Chatterjee, "Swept-source optical coherence tomography of lower limb wound healing with histopathological correlation," J. Biomed. Opt. 16, 0260101–0260108 (2011).
- [13] K. Fukunaga, Introduction to Statistical Pattern Recognition (Academic Press, 2nd ed., New York, 1990).